AFRL-AFOSR-VA-TR-2016-0124

Reduced Heat Flux Through Preferential Surface Reactions Leading to Vibrationally and Electronically Excited Product States

Thomas Schwartzentruber
REGENTS OF THE UNIVERSITY OF MINNESOTA MINNEAPOLIS

03/04/2016
Final Report

Air Force Research Laboratory
AF Office Of Scientific Research (AFOSR)/ RTB2
Arlington, Virginia 22203
Air Force Materiel Command

REPORT DOCUMENTATION PAGE

Form Approved
OMB No. 0704-0188

PLEASE DO NOT RETURN YOUR FORM TO THE ABOVE ORGANIZATION.

1. REPORT DATE *(DD-MM-YYYY)*	2. REPORT TYPE	3. DATES COVERED *(From - To)*
27-02-2016	Final Report	09/30/2012 -11/30/2015

4. TITLE AND SUBTITLE
Reduced Heat Flux Through Preferential Surface Reactions Leading to Vibrationally and Electronically Excited Product States

5a. CONTRACT NUMBER
FA9550-12-1-0486

5b. GRANT NUMBER

5c. PROGRAM ELEMENT NUMBER

6. AUTHOR(S)
Schwartzentruber, Thomas, E.

5d. PROJECT NUMBER

5e. TASK NUMBER

5f. WORK UNIT NUMBER

7. PERFORMING ORGANIZATION NAME(S) AND ADDRESS(ES)
Regents of the University of Minnesota
Office of Sponsored Projects Admin
200 Oak St. SE
Minneapolis, MN 55455

8. PERFORMING ORGANIZATION REPORT NUMBER

9. SPONSORING/MONITORING AGENCY NAME(S) AND ADDRESS(ES)
AF Office of Scientific Research
875 N Randolph St., Rm 3112
Arlington, VA 22203

10. SPONSOR/MONITOR'S ACRONYM(S)

11. SPONSOR/MONITOR'S REPORT NUMBER(S)

12. DISTRIBUTION/AVAILABILITY STATEMENT
A - Approved for public release.

13. SUPPLEMENTARY NOTES

14. ABSTRACT
Instead of characterizing a hypersonic flight environment and then selecting an appropriate thermal protection system (TPS) that can survive the environment, it would be a significant technological step forward if the TPS could be engineered to alter the hypersonic flight environment itself (i.e. the boundary layer). A critical aspect of such a strategy is control over energy deposition pathways during catalytic recombination of dissociated air species on TPS surfaces. Experiments with laser-based diagnostics were used to simultaneously measure the loss of oxygen atoms and the production of oxygen molecules in the ground and electronically excited states as a partially dissociated oxygen flow interacts with a silica surface. Flow models were constructed and numerical calculations were performed to interpret the experimental data. New computational chemistry approaches, capable of modeling nonadiabatic oxygen interactions (electronically excited interactions) with surface defects, were developed. Through such computational chemistry modeling we determined precisely how and why such excited-state molecules are produced, by determining the specific silica defects and reaction pathways that are responsible.

15. SUBJECT TERMS
High temperature gas-surface interactions
Molecular Dynamics
Computational Fluid Dynamics

16. SECURITY CLASSIFICATION OF:			17. LIMITATION OF ABSTRACT	18. NUMBER OF PAGES	19a. NAME OF RESPONSIBLE PERSON
a. REPORT	b. ABSTRACT	c. THIS PAGE			Thomas Schwartzentruber
UU	UU	UU	UU	24	19b. TELEPHONE NUMBER *(Include area code)* 612-625-6027

Reset

Standard Form 298 (Rev. 8/98)
Prescribed by ANSI Std. Z39.18
Adobe Professional 7.0

INSTRUCTIONS FOR COMPLETING SF 298

1. REPORT DATE. Full publication date, including day, month, if available. Must cite at least the year and be Year 2000 compliant, e.g. 30-06-1998; xx-06-1998; xx-xx-1998.

2. REPORT TYPE. State the type of report, such as final, technical, interim, memorandum, master's thesis, progress, quarterly, research, special, group study, etc.

3. DATES COVERED. Indicate the time during which the work was performed and the report was written, e.g., Jun 1997 - Jun 1998; 1-10 Jun 1996; May - Nov 1998; Nov 1998.

4. TITLE. Enter title and subtitle with volume number and part number, if applicable. On classified documents, enter the title classification in parentheses.

5a. CONTRACT NUMBER. Enter all contract numbers as they appear in the report, e.g. F33615-86-C-5169.

5b. GRANT NUMBER. Enter all grant numbers as they appear in the report, e.g. AFOSR-82-1234.

5c. PROGRAM ELEMENT NUMBER. Enter all program element numbers as they appear in the report, e.g. 61101A.

5d. PROJECT NUMBER. Enter all project numbers as they appear in the report, e.g. 1F665702D1257; ILIR.

5e. TASK NUMBER. Enter all task numbers as they appear in the report, e.g. 05; RF0330201; T4112.

5f. WORK UNIT NUMBER. Enter all work unit numbers as they appear in the report, e.g. 001; AFAPL30480105.

6. AUTHOR(S). Enter name(s) of person(s) responsible for writing the report, performing the research, or credited with the content of the report. The form of entry is the last name, first name, middle initial, and additional qualifiers separated by commas, e.g. Smith, Richard, J, Jr.

7. PERFORMING ORGANIZATION NAME(S) AND ADDRESS(ES). Self-explanatory.

8. PERFORMING ORGANIZATION REPORT NUMBER. Enter all unique alphanumeric report numbers assigned by the performing organization, e.g. BRL-1234; AFWL-TR-85-4017-Vol-21-PT-2.

9. SPONSORING/MONITORING AGENCY NAME(S) AND ADDRESS(ES). Enter the name and address of the organization(s) financially responsible for and monitoring the work.

10. SPONSOR/MONITOR'S ACRONYM(S). Enter, if available, e.g. BRL, ARDEC, NADC.

11. SPONSOR/MONITOR'S REPORT NUMBER(S). Enter report number as assigned by the sponsoring/ monitoring agency, if available, e.g. BRL-TR-829; -215.

12. DISTRIBUTION/AVAILABILITY STATEMENT. Use agency-mandated availability statements to indicate the public availability or distribution limitations of the report. If additional limitations/ restrictions or special markings are indicated, follow agency authorization procedures, e.g. RD/FRD, PROPIN, ITAR, etc. Include copyright information.

13. SUPPLEMENTARY NOTES. Enter information not included elsewhere such as: prepared in cooperation with; translation of; report supersedes; old edition number, etc.

14. ABSTRACT. A brief (approximately 200 words) factual summary of the most significant information.

15. SUBJECT TERMS. Key words or phrases identifying major concepts in the report.

16. SECURITY CLASSIFICATION. Enter security classification in accordance with security classification regulations, e.g. U, C, S, etc. If this form contains classified information, stamp classification level on the top and bottom of this page.

17. LIMITATION OF ABSTRACT. This block must be completed to assign a distribution limitation to the abstract. Enter UU (Unclassified Unlimited) or SAR (Same as Report). An entry in this block is necessary if the abstract is to be limited.

Reduced Heat Flux Through Preferential Surface Reactions Leading to Vibrationally and Electronically Excited Product States

FINAL TECHNICAL REPORT: Grant #FA9550-12-1-0486

2013 Basic Research Initiative (BRI) – BAA-AFOSR2012-0001
Foundations of Energy Transfer in Multi-Physics Flow Phenomena
United States Air Force Office of Scientific Research

Lead PI:
Prof. Thomas E. Schwartzentruber
Aerospace Engineering and Mechanics,
University of Minnesota

Phone: 612-625-6027 Fax: 612-626-1558 Email: schwart@umn.edu

Co-PIs: Prof. Don Truhlar (University of Minnesota)
Dr. Jochen Marschall (SRI Intl.)
Dr. Jason White (SRI Intl.)

ABSTRACT

Instead of characterizing a hypersonic flight environment and then selecting an appropriate thermal protection system (TPS) that can survive the environment, it would be a significant technological step forward if the TPS could be engineered to alter the hypersonic flight environment itself (i.e. the boundary layer). A critical aspect of such a strategy is control over energy deposition pathways during catalytic recombination of dissociated air species on TPS surfaces. The first objective of this work was to design an experimental setup and perform definitive experimental evaluation of the production of excited oxygen molecules resulting from oxygen-atom surface recombination. In these experiments laser-based diagnostics were used to simultaneously measure the loss of oxygen atoms and the production of oxygen molecules in the ground and electronically excited states as a partially dissociated oxygen flow interacts with a silica surface. The second objective was to construct flow models and perform numerical calculations to interpret the experimental data. The third objective was to develop new computational chemistry approaches capable of modeling the challenging problem of nonadiabatic oxygen interactions (electronically excited interactions) with specific catalytic defects found on real silica surfaces. Through such computational chemistry modeling we determined precisely how and why such excited-state molecules are produced, by determining the specific silica defects and reaction pathways that are responsible.

POINT-BY-POINT SUMMARY:

What have we learned from this project?

1. The Structure of High Temperature Silica Surfaces
Through computational chemistry and existing experimental literature, we have determined the precise surface defects involved in atomic oxygen recombination on silica surfaces (quartz and amorphous SiO_2) at high temperature.

2. Electronic Structure Calculations of Atomic Oxygen Recombination at Surface Defects:
Through computational chemistry we have determined the atomic configurations of these defects, discovered that their energetics are highly localized enabling the use of accurate quantum chemical theory, and determined the reaction profiles for atomic oxygen recombination on these defects.

3. Reaction Profiles for Atomic Oxygen Recombination are Barrierless
We have determined that these defects enable an autocatalytic cycle for oxygen recombination on silica surfaces, and most importantly, that this cycle is barrierless (no activation energies). To our knowledge, all existing finite-rate recombination models assume an activated (and therefore temperature dependent) process.

4. Manifolds of Low-Lying Electronic States and Potential Energy Surfaces
Through computational chemistry we have determined all of the low-lying electronic energy states associated with the defect structures. It is clear that there are many possible doublet potential energy curves leading to the excited states of O_2 in the atomic oxygen recombination reaction. Such reactions were confirmed experimentally during this project (see 6-8 below).

5. Boundary Layer Analysis (DSMC) and Vibrational Energies of Product Molecules
Through computational chemistry we have determined that oxygen recombines into vibrationally excited states (approximate analysis found $\nu = 8$ being most probable). However, through direct simulation Monte Carlo (DSMC) calculation we have found that, under hypersonic conditions of interest, this vibrational energy is rapidly deposited into the boundary layer gas (translational modes) through collisional processes, and transferred back to the surface. Therefore, we conclude that the vibrational energy states of recombined molecules have little effect on the overall heat flux to a surface. However, if the flow is locally rarefied (i.e. sharp leading edges at higher altitudes), vibrational energy accommodation may influence the overall heat flux.

6. Experimental Verification of Recombination into Electronically Excited O_2
We have detected, and quantified, oxygen-silica surface recombination producing molecular oxygen in its first electronically excited state, $O_2(a^1\Delta g)$, by performing experiments of atomic oxygen flow through a fused-quartz tube at high-temperature. We infer from the experimental data that approximately $1/10^{th}$ of all recombination reactions produce $O_2(a^1\Delta g)$.

7. Flow Modeling and Quantification of the $O_2(a^1\Delta g)$ Production Rate
In order to infer reaction production efficiencies from the optical diagnostic measurements we developed a reacting flow model to characterize the experimental flow environment. In addition

to the conclusion that $1/10^{th}$ of all recombination reactions produce $O_2(a^1\Delta g)$, the combination of experimental data and flow modeling revealed that *quenching* of $O_2(a^1\Delta g)$, back into the ground state of O_2 due to surface collisions, is highly probable. This is an important result that suggests that even if significant energy is carried away from the surface in the electronic energy of recombined molecules, this energy is likely to be deposited back to the surface.

8. Experimental Detection of Recombination into the 2nd Electronically Excited State of O_2
By performing further experiments of atomic oxygen flow through a fused-quartz tube at high-temperature, we have also measured molecular oxygen production, resulting from surface recombination, in both the ground state and the second electronically excited state $O_2(b^1\Sigma g^+)$. These measurements are qualitatively consistent with the computational chemistry predictions (see 4 above).

Each of these points (1-8) is discussed in detail in this report.

PUBLICATIONS:

Book Chapter:

Jochen Marschall, Matthew MacLean, Paul E. Norman, and Thomas E. Schwartzentruber,
Hypersonic Nonequilibrium Flows: Fundamentals and Recent Advances
Chapter 6: Surface Chemistry in Nonequilibrium Flows,
Progress in Astronautics and Aeronautics, Volume 247, AIAA 2015.
http://dx.doi.org/10.2514/5.9781624103292.0239.0328

Articles:

[1] Paneda, R.M., Paukku, Y., Duanmu, K., Norman, P., Schwartzentruber, T.E., and Truhlar, D.G., "Atomic Oxygen Recombination at Surface Defects on Reconstructed (0001) α-Quartz Exposed to Atomic and Molecular Oxygen", *J. Phys. Chem. C* (2015), 119, pp. 9287-9301.

[2] Norman, P., Schwartzentruber, T.E., Leverentz, H., Luo, A., Paneda, R.M., Paukku, Y., and Truhlar, D.G., "The Structure of Silica Surfaces Exposed to Atomic Oxygen", *J. Phys. Chem. C* (2013), 117, pp. 9311-9321.

[3] "Singlet Molecular Oxygen Formation by O-atom Recombination on Fused Quartz Surfaces", by J. D. White, R. A. Copeland, and J. Marschall, *Journal of Thermophysics and Heat Transfer*, **29,** No.1, pp. 24-36. January-March 2015.

[4] Schwartzentruber, T.E., Poovathingal, S., and Stern, E.C., "Molecular Simulation of Oxygen Reactions with Realistic Carbon and Silica Surfaces at High Temperature", *AIAA Paper 2015-3567*, July 2015, presented at the 20th AIAA International Space Planes and Hypersonic Systems and Technologies Conference, Glasgow, Scotland.

[5] Schwartzentruber, T.E., Poovathingal, S., and Stern, E.C., "Molecular Simulation of Oxygen Reactions with Realistic Silica and Carbon Surfaces at High Temperature", *Proceedings of the 8th European Symposium on Aerothermodynamics*, European Space Agency, 2015, id.84668, Lisbon, Portugal.

[6] White, Jason D., Richard A. Copeland, and Jochen Marschall. "Singlet O2 Formation by O-atom Recombination on Fused Quartz Surfaces." *AIAA Paper 2014-0515,* 52nd Aerospace Sciences Meeting. National Harbor, Maryland, 2014.

[7] "Empirical potential for modeling ground-state chemical reactions between energetic oxygen atoms and defects at silica surfaces and its use to study Eley-Rideal reactions," M. A. Makeev, K. Duanmu, R. Meana-Pañeda, and D. G. Truhlar, 2016, in preparation.

DETAILED TECHNICAL RESULTS OF THE PROJECT:

1. The Structure of High Temperature Silica Surfaces

In this work we began by using molecular dynamics simulations with the $ReaxFF_{SiO}^{GSI}$ potential to identify the chemical surface structures and defects on both quartz and amorphous silica exposed to atomic oxygen at high temperature. The $ReaxFF_{SiO}^{GSI}$ potential was specifically fit to data from a large number of electronic structure calculations under a previous AFOSR grant, and all details are contained in the following publication:

Kulkarni, A.D., Truhlar, D.G., Srinivasan, S.G., van Duin, A.C.T., Norman, P., and Schwartzentruber, T.E., "**Oxygen Interactions with Silica Surfaces: Coupled Cluster and Density Functional Investigation and the Development of a New ReaxFF Potential**", *J. Phys. Chem. C* (2013), 117, pp. 258-269.

Unlike surfaces created from crystalline bulk materials, annealed amorphous SiO_2 surfaces contain a finite number of catalytic defects (surface sites where catalytic events may be energetically favorable). However, these defects may change in number or in chemical structure when exposed to a high temperature dissociated gas, as may be the case in air plasma experiments and hypersonic flight. In order to simulate exposure to atomic oxygen, we used MD simulations with a novel Flux Boundary Condition (FBC); a method that exposes a surface to an ideal gas at a given temperature, pressure, and composition. A more detailed description of this method can be found in:

Norman, Schwartzentruber, T.E., and Cozmuta, I., "**A Computational Chemistry Methodology for Developing an Oxygen-Silica Finite Rate Catalytic Model for Hypersonic Flows**", *AIAA Paper 2011-3644*, June 2011, presented at the 42nd AIAA Thermophysics Conference, Honolulu, HI.

In Flux Boundary Condition simulations, atoms are generated at random points on a plane above the surface with a frequency corresponding to the flux of an ideal gas through that plane. This plane is 10 Angstroms above the surface, beyond the force cutoff of the potential. Impinging atoms are given velocities sampled from a Maxwell-Boltzmann distribution and a random incident angle. Atoms or molecules moving away from the surface at a distance greater than 10 Angstroms are deleted, allowing us to simulate only the gas-surface interface region, and gas phase collisions in this region are rare. A diagram of this method is shown in Fig 1(a). Over the course of a simulation, gas atoms adsorb on the initially empty surface, which eventually reaches a steady state population of adsorbed atoms as seen in Fig. 1(b). At steady state we can determine the concentration and nature of chemical defects for an amorphous SiO_2 surface exposed to a dissociated gas at a given temperature and pressure. Examples of steady state surfaces for both amorphous SiO_2 and crystalline SiO_2 (quartz) are shown in Figs. 2(a) and 2(b), respectively.

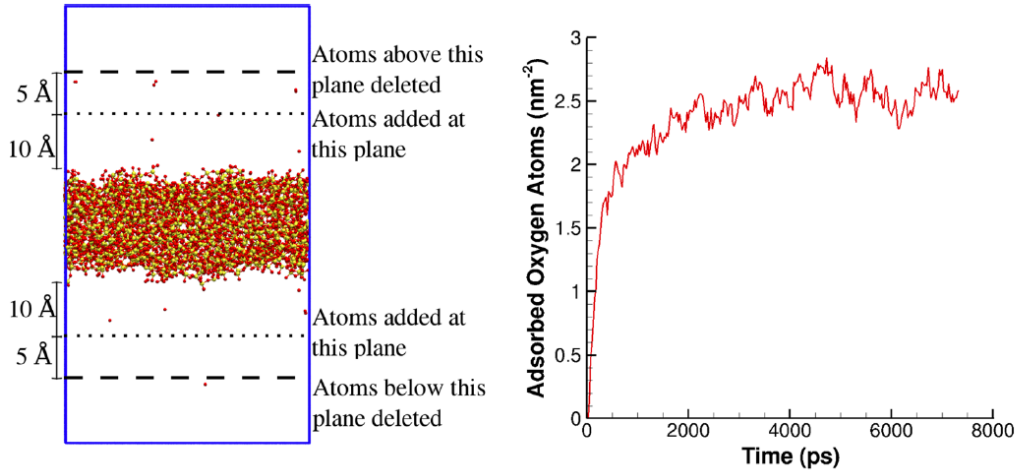

(a) Diagram of the flux boundary condition

(b) Concentration of adsorbed oxygen vs. time for a-SiO_2 surface at 10 atm, 1000 K

Figure 1: Depiction of the Flux Boundary Condition technique to predict surface structure under exposure to a high-temperature dissociated oxygen gas.

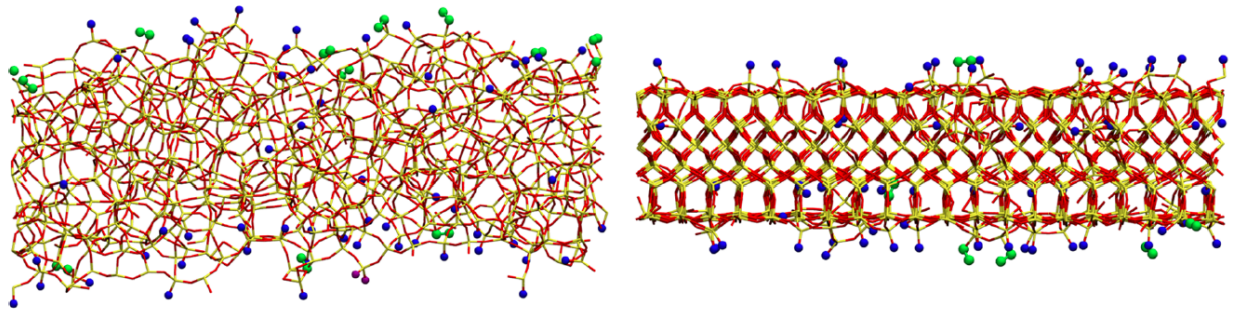

(a) a-SiO_2 slab

(b) Reconstructed (0001) α-quartz slab

Figure 2: Defects on silica surfaces after exposure to atomic oxygen. Defects are highlighted with colored spheres: NBO I (blue), NBO III (purple), peroxyl (green).

Only a small number of distinct defect chemistries were observed in the simulations. These are shown in Fig. 3 below. We found that the most frequently occurring surface defects were a nonbridging oxygen atom defect (NBO I) and a peroxyl defect. Based on the binding energy of the oxygen atoms at these sites, we showed that both are potentially chemically active with respect to Eley-Rideal recombination. There is experimental evidence for the existence of these defects on mechanically ground and irradiated silica surfaces at low temperatures. We demonstrated that the structure of the peroxyl defect as predicted by the $ReaxFF_{SiO}^{GSI}$ potential agrees reasonably well with DFT calculations, despite the fact that the peroxyl defect was not included in the training set of the $ReaxFF_{SiO}^{GSI}$ potential. However, the $ReaxFF_{SiO}^{GSI}$ potential underpredicts the binding energy of the O_2 molecule on this defect by 0.9 eV. Results of molecular dynamics simulations for surfaces exposed to atomic oxygen at a high gas-phase pressure of 10 atm showed that the total concentration of defects on quartz and a-SiO_2 slabs (for example refer to Fig. 2) did not vary significantly with temperature. The total concentration of defects on the a-SiO_2 surface did increase noticeably with pressure over the pressure range 1− 15 atm at a temperature of 1500 K. The gas-phase pressures used in MD simulations were several orders of magnitude higher than those used in many experimental setups, so no quantitative

conclusions about the total concentration of defects on silica surfaces under experimental conditions can be drawn. However, our research concluded that the *types* of surface defects predicted by the simulations (Fig. 5) do not change with pressure, rather the same types of defects are seen consistently on both amorphous and quartz surfaces under a range of conditions.

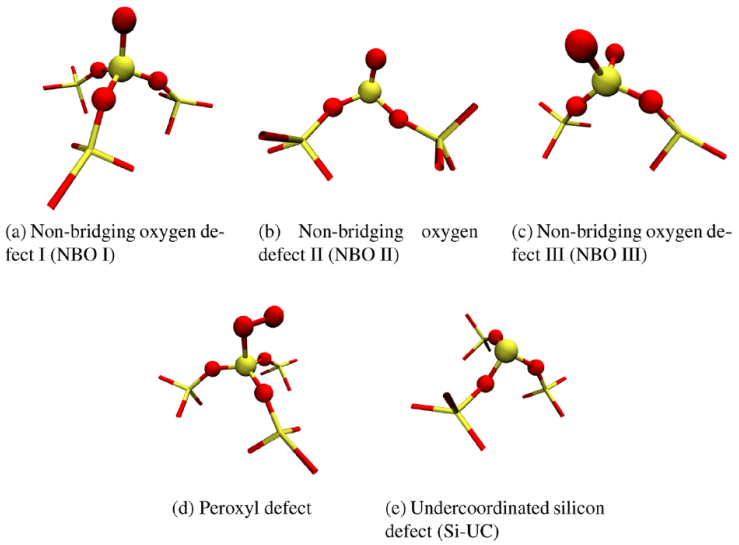

Figure 3: Surface defects. Oxygen atoms (red). Silicon atoms (yellow).

In terms of the structure of silica surfaces, we conclude that the defects predicted by our MD simulations are present on real silica surfaces exposed to dissociated oxygen at high temperatures, representative of surface conditions during hypersonic flight. The chemistry of the predicted surface structures is supported by density functional theory calculations, and the existence of such defects on silica surfaces is consistent with available experimental data. These defects provide a feasible pathway for the catalytic recombination of atomic oxygen. Thus, the next aspect of the project focuses on studying these specific active surface sites using electronic structure calculations to determine highly accurate binding energies and transition state energies for building chemical rate models of high-temperature oxygen-silica catalytic recombination.

2. Electronic Structure Calculations of Atomic oxygen recombination at surface defects:

We then proceeded to study the nature of defects exposed to atomic and molecular oxygen. We employed quantum mechanical electronic structure calculations to study an uncoordinated silicon defect, a non-bridging oxygen defect, and a peroxyl defect. We characterized the spin states and energies of the defects, and calculated the reaction profiles for atomic oxygen recombination at the defects. We elucidated the diradical character by analyzing the low-lying excited states using multireference configuration interaction methods. We showed that the diradical defects consist of weakly coupled doublet radicals, and that atomic oxygen recombination can take place through a barrierless process at defects. We have delineated the recombination mechanism and computed the formation energy of the peroxyl and non-bridging oxygen defects. *We found that key recombination reaction paths are barrierless.* In addition, we characterized the electronically excited states that may play a role in the chemical and physical processes that occur during recombination on these surface defect sites.

We use cluster models to study the surfaces. First we describe the way that we created the cluster models of defects; then we describe the electronic structure methods.

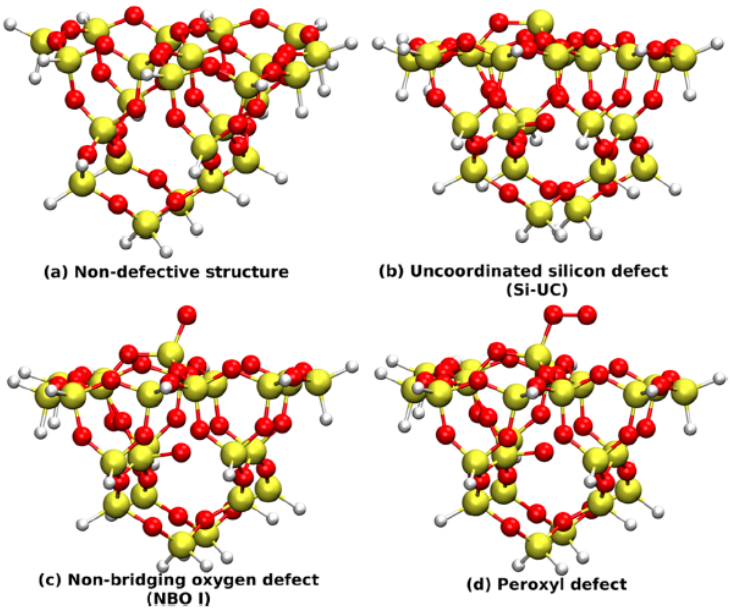

Figure 4: Cluster models used for electronic structure calculations. T24 models are depicted.

A reconstructed quartz surface was created by following the recipe described in section 3.1 of our journal article [2]. A 2401-atom periodic cluster of the reconstructed quartz surface that contains one central peroxyl defect was energy minimized by using the $ReaxFF_{SiO}^{GSI}$ potential. From this structure, we generated a cluster that contains 24 atoms of Si, called here T24 (which denotes that it has 24 silicon atoms, all tetrahedral (T) centers in the nondefective structure); this is the starting point for the generation of smaller clusters explained below. Figure 4(a) shows the T24 cluster model for the nondefective structure. The T24 cluster for the NBO I defect was generated as follows: three spheres with a radius of 6 Å were created around the three key atoms, the central silicon atom and the two uncoordinated oxygen atoms of the NBO I defect (see Figure 4(c)). All atoms within the spheres, or involved in the 12 membered rings that include any of the atoms inside the spheres, were retained. The under-coordinated silicon atoms were capped with hydrogen atoms (with a fixed Si− H distance of 1.46 Å) to restore proper coordination of the model. A partial optimization of the cluster model was then carried out by optimizing all atoms within a radius of 4 Å from any of the three key atoms. The same atoms and atomic positions were used with the same procedure for generating and energy minimizing the T24 nondefective structure, the Si-UC defect, and the peroxyl defect. Figure 4 shows the T24 structures for the three defects to be studied in this article: Si-UC (Fig. 4(b)), NBO I (Fig. 4(c)), and peroxyl (Fig. 4(d)) defects.

Other smaller clusters that mimic the atomic structure of the defects shown in Fig. 4 were also considered in this study. We use the notation T**n**x where **n** represents the number of Si atoms in the cluster, and x is “a” or “b”. Here “a” is when each Si is terminated by 3 H atoms, whereas “b” is when each Si is bonded to 3 O atoms, each of which are terminated by 1 H atom. All details can be found in our journal paper [1].

Kohn−Sham density functional theory was used for geometry optimization of all of the models and to study the mechanism of atomic oxygen recombination on the surface defects. The state-averaged complete active space self-consistent field (CASSCF) method followed by the multireference configuration interaction MRCISD+Q method is used for the calculation of the

excited states in the study of the diradical character of the defects and to map out the excited states at some reaction-path geometries.

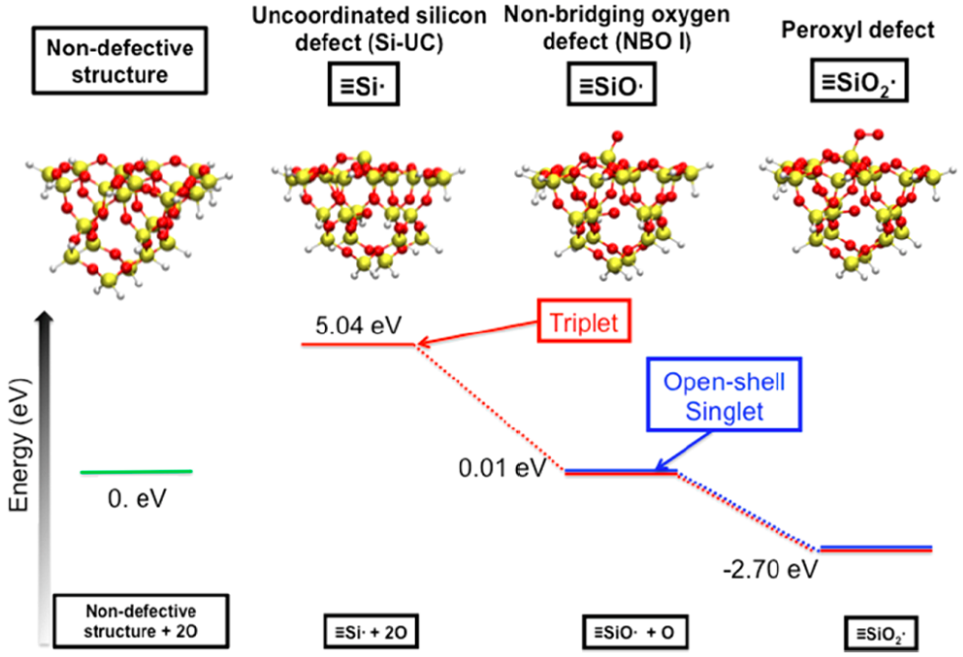

Figure 5: Relative energies (in eV) of electronic states of various spin for nondefective structure and three defects of the silica surface using cluster model T24 at the M06-L/6-311G(2d,d) level of theory. Note that open-shell singlet (blue lines) and triplet (red lines) almost coincide for the NBO I and peroxyl defets, so the blue-and-red energy level corresponds to both of the states in those cases.

Figure 5 presents the results of the electronic structure calculations for the nondefective structure and the Si-UC, NBO I, and peroxyl defects, as obtained using the T24 cluster. Using the procedures described above, the geometries of the nondefective and defective structures were partially relaxed by M06-L/6-311G(2d,d). All structures of T24 have an even number of electrons; they are closed-shell singlets (nondefective structure) or diradicals (defective structures). For the diradicals, two electronic spin states have been considered, a triplet and a broken-symmetry open-shell singlet. The energetic profile depicted in Fig. 5 shows the relative stability of various structures with respect to the nondefective ground electronic state, which corresponds to a closed-shell singlet electronic state. Note that to obtain these relative energies, the energy of one or two atoms of ground-state oxygen (depending on the structure) was added to the energy of the corresponding system, because a meaningful comparison of energies requires that the energies correspond to the same number of atoms with atomic number. The closed-shell singlet ground state for the nondefective structure (plus two ground-state oxygen atoms) has been taken as the zero of energy (see Fig. 5). The nondefective structure has a singlet ground state, but we found that all three defective structures have a triplet ground state. In every case, we also tried to optimize the geometry for an open-shell singlet by using the broken-symmetry method. For the NBO I and peroxyl defects, this led to a stable structure, with a geometry nearly the same as that corresponding to the triplet, and with the singlet energy slightly higher. The spin contamination in the open-shell singlet is large, having the values of 1.0093 and 1.0086 for the expectation value of the square of the total electron spin ($\langle \mathbf{S}^2 \rangle$) for the NBO I and peroxyl

defects, respectively; this indicates that these broken symmetry states are mixtures of the singlet and triplet, but because the energies of the singlet and the triplet are nearly the same, we need not take linear combinations to resolve the singlet component. For the Si-UC defect, the open-shell singlet does not correspond to a stable structure on the potential energy surface.

The minimum-energy geometry on the triplet surface of the Si-UC defect is 5.04 eV higher in energy than the singlet energy of the nondefective structure. Its geometry differs from the nondefective structure in two main ways: (i) the bond between the central silicon atom and one of its corresponding bonded oxygens (located in a deeper layer) is broken, and (ii) a pyramidal inversion of the central silicon atom. Fig. 5 shows that the peroxyl defect is calculated to be the most stable structure, and this finding agrees with the fact that the NBO I and peroxyl defects were the most common defects observed in previous journal article [2]; we believe therefore that the peroxyl defect is an important structure for understanding the catalytic recombination of oxygen atoms on the silica surface. To study the dynamics of the atomic oxygen recombination catalyzed on these defects and to propose new models to study it, we had to answer some further questions, for example: How strong is the interaction between monoradicals in the diradical structures? What kind of models can be used to study the dynamics of the atomic oxygen recombination? Do we need to consider excited states in addition to the states shown in Fig. 5? How does the interaction between radicals influence the energy differences between the excited electronic states? All of these questions are answered in our journal article [1], and are now summarized briefly.

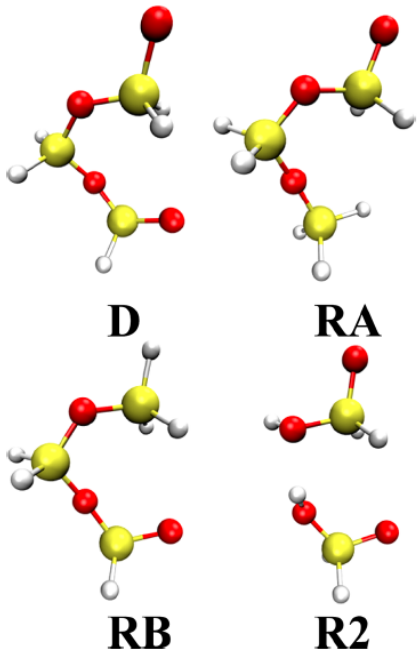

Figure 6: Models used to study the diradical nature of the NBO I defect.

One important result of the electronic structure calculations was the finding that the diradical defects consist of weakly coupled doublet radicals. That is, the defects are highly localized and can therefore be studied in precise detail. This is depicted in Fig. 6. The result that all nine low-lying states of the diradical molecule D could be simply reproduced by calculating single radical molecules RA and RB, further confirms that the two local radicals of D are separable. This provides a useful strategy for modeling defects in simulations; that is, they can be modeled as localized defects that interact only weakly, and we will use this conclusion in the next section.

3. Reaction Profiles for Atomic Oxygen Recombination are Barrierless

In this section, we present the reaction profiles for atomic oxygen recombination on the silica surface defects.

The relative energies calculated by M06/MG3S for various size models of the defects are shown in Fig. 7. The energies converge nicely as the size of the cluster increases (e.g., the difference in the relative energies between models T4a and T4b is less than 1%), and they are in good agreement with the values obtained for the diradical T24 cluster model (see Fig. 5).

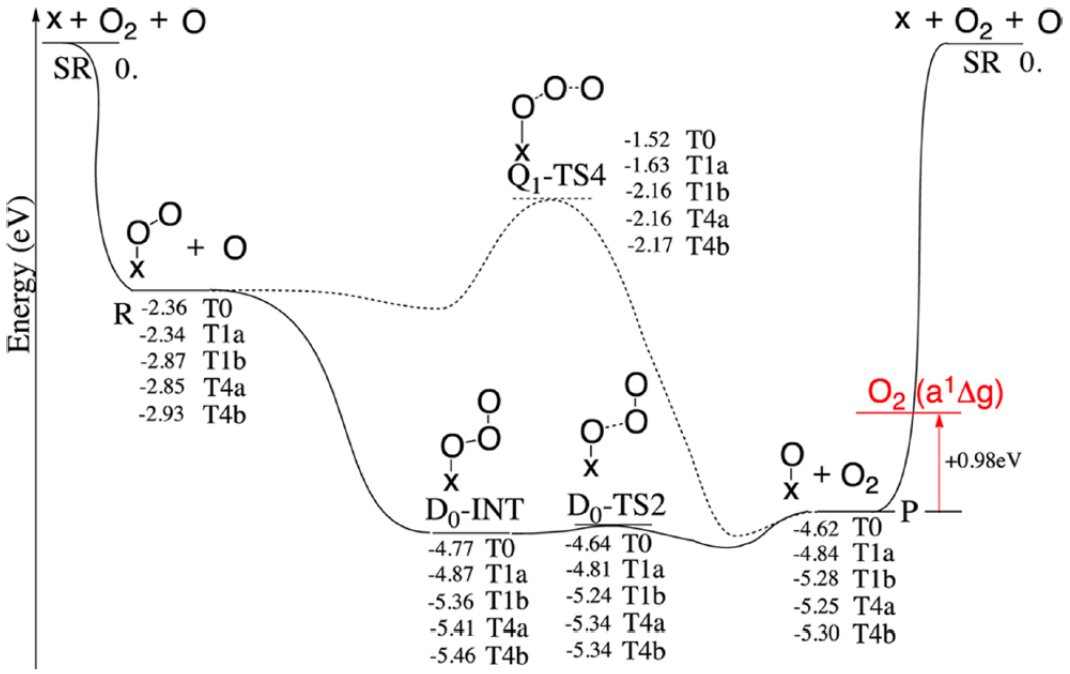

Figure 7: Reaction profile for the atomic oxygen recombination using various models obtained with M06/MG3S model chemistry. X denotes the silica surface. The energies shown all correspond to the overall system, including separate atoms and diatoms when indicated. The energy levels shown at **SR** and **R** are the same for the overall doublet state and the overall triplet state, but after that the paths diverge with the doublet being lower; at P the lowest overall doublet and lowest overall quartet again have the same energy.

In terms of a mechanism for the recombination of atomic oxygen, Fig. 7 implies that one peroxyl defect and one atom of oxygen can lead to a NBO I defect and one molecule of oxygen. Figure 7 shows this in more detail by presenting the entire profile of reaction for the models T**x**a/b (with **x**=1 or **x**= 4) by using the M06/MG3S model chemistry. In a first step, the peroxyl defect forms an intermediate product, labeled here as **D_0-INT** (where D_0 denotes that the spin state of the system is a doublet). Our calculations indicate that this reaction is barrierless.

In a second step, the intermediate **D_0-INT** produces the molecule of oxygen through the transition state, **D_0-TS2** , which has small barrier height, about 0.06 eV. Adding atomic oxygen to one of the products of reaction (i.e., the NBO I defect), the peroxyl defect can be regenerated. This step closes an autocatalytic cycle that catalyzes the atomic oxygen recombination. We have also included the reaction channel for the first excited state, which is a quartet spin state; this is a concerted reaction passing through the transition state **Q_1-TS4**. These results are a first in the literature and clearly show a barrierless oxygen recombination pathway involving defects on silica surfaces. To our knowledge all existing models for oxygen recombination on silica surfaces assume an activated process, and therefore a surface temperature dependent reaction rate. Our findings will change the way the way this process is modeled in simulations involving high temperature gas-surface chemistry.

In addition, the energy required to access the first electronically excited state of oxygen $O_2(a^1\Delta g)$, is shown in Fig. 7. Clearly, this exothermic surface recombination reaction has

sufficient energy that recombined oxygen molecules leave the surface in the $O_2(a^1\Delta g)$ state. During this project we experimentally verified the creation of significant $O_2(a^1\Delta g)$ through surface recombination reactions. This is a second discovery that will change the way oxygen recombination is modeled in simulations involving high temperature gas-surface chemistry.

4. Manifolds of Low-Lying Electronic States and Potential Energy Surfaces

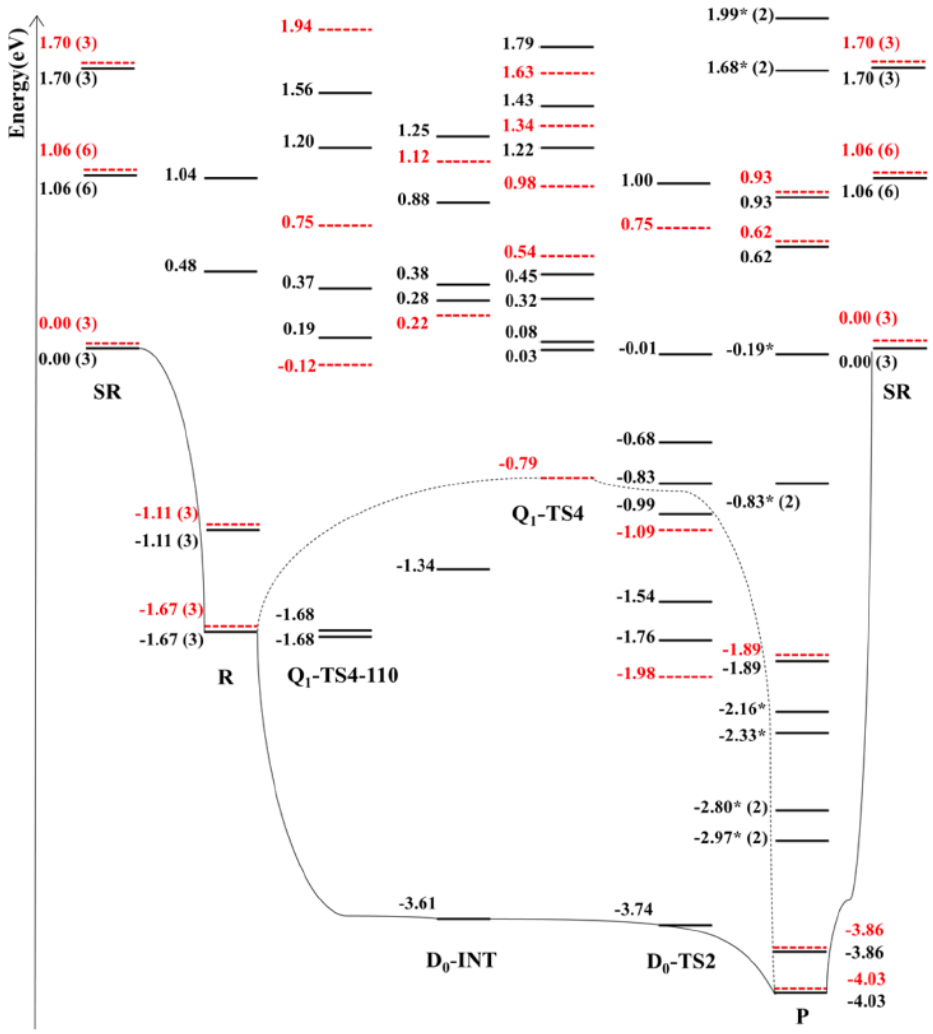

Figure 8: Reaction profile for atomic oxygen recombination using the T1a model obtained with MRCISD+Q/6-311G(2d,d) single point calculations on M06/MG3S geometries. Doublet and quartet states within 2eV of the ground state of **SR** are shown. The lowest doublet and quartet reaction pathways are represented by curved lines and dashed curved lines. A black solid line denotes a doublet spin state, and a red dashed line denotes a quartet spin state; the number in parenthesis is the degeneracy of the state, and the asterisk means the state involves O_2 in an excited state.

The experiments described later in sections 6, 7, and 8 have demonstrated significant production of molecular oxygen in its first excited state, $O_2(a^1\Delta g)$. To understand the mechanism of $O_2(a^1\Delta g)$ formation, we next calculated the low-lying excited states using the T1a model. The reaction profile with all low-lying doublet and quartet states (states below 2 eV) for the atomic

oxygen recombination reaction is shown in Fig. 8. Figure 8 shows a large number of energy levels within 2 eV of the ground state of **SR**. For the species **P**, all states that consist of O_2 in excited state are marked with asterisks, including states at − 2.97, − 2.80, − 0.83, 1.68, and 1.99 eV involving $O_2(a^1\Delta g)$ and states at − 2.16, − 2.33, and − 0.19 eV involving $O_2(b^1\Sigma g+)$, the second excited state of molecular oxgyen. These states are all in the doublet spin manifold. With all of the low-lying states in the Fig. 8, it is clear that there are many possible doublet potential energy curves leading to the excited states of O_2 in the atomic oxygen recombination reaction. Dynamics calculations would be quite interesting, and they could be carried out using a method suitable for a dense manifold of excited states. This is discussed next.

It is well established that most empirical potentials developed for solid-state materials have only a limited capability in describing chemical reactions on surfaces – in fact, even a quantitative description of nonreactive surface properties of solid materials is challenging. Therefore, it is of great essence to develop empirical models that refine conventional approaches to interatomic potential design to allow a more treatment of chemical reactions on surfaces of extended materials. We have embarked upon designing a new framework that incorporates the essential description of chemical reactions between silica-surface defects and impinging oxygen atoms into a traditional empirical potential scheme.

Our framework is similar in some respects to well-known embedded cluster methods; however, it does not require any quantum mechanical calculations to be performed during the classical simulation procedure. The latter feature is important for making the approach computationally feasible. The approach developed by us is based on separation of the bulk and defect characteristics of silica; the former are described by the Tersoff potential, the latter part includes all the interactions specific for defects and can be called an O-defect potential (note that the present framework focuses on the interactions of silica only with oxygen atoms although it is extendable to other target-projectile realizations). Whilst the Tersoff potential is conventionally used for atomistic simulations of silica and other silicon- as well as carbon-based materials, a novel approach is employed for defect clusters description.

The description is based on the natural bond order concept. It is designed to reproduce the changes in interaction parameters and structural modifications in surface-defect clusters, by functional forms involving the change in numbers of nearest neighbors (treated as continuous variables) around each atom of the extended defect. The interaction between impinging oxygen atoms and an extended defect is described by varying both the structural and energetic properties of the cluster as functions of the distance between the arriving oxygen atom and atoms comprising the defect. This is achieved by making all the parameters of the interaction potential continuous functions of the corresponding numbers of nearest neighbors. A central concept in the approach is the use of the Wiberg bond order matrix. Local Wiberg matrices are extracted directly from the quantum-chemistry (ab initio) calculations and, correspondingly, the potential, describing the defects, can be considered as a semi-quantum approximation. The Wiberg indexes (matrix elements) allow one to extract the energies associated with each bond in a cluster from the cluster's total energy. Thus, the contribution of a bond to the total energy changes with both bond-length and number of nearest neighbors. Therefore, an arriving atom forms a bond with a defect atom following the path "prescribed" by the quantum calculations – in what relates to both micro-structural properties and energetics. The present approach is designed to treat a few selected surface-defect types only. Those types were identified and described in our journal article [2]. One of the main virtues of the already developed framework must particularly be

emphasized. That is, unlike more general methods, the present approach is extendable to include excited-state configurations. A journal article on this work is in preparation:

"Empirical potential for modeling ground-state chemical reactions between energetic oxygen atoms and defects at silica surfaces and its use to study Eley-Rideal reactions," M. A. Makeev, K. Duanmu, R. Meana-Pañeda, and D. G. Truhlar, in preparation, 2016.

5. Boundary Layer Analysis (DSMC) and Vibrational Energies of Product Molecules

In addition to recombination into electronically excited states, there is ample energy available to recombine into vibrationally excited states. Computational chemistry work from prior years indicated that recombination reactions occurring on the peroxyl defect site (the main reaction site) have a high probability of leaving the surface in a vibrationally excited state. Figure 9 shows results of molecular dynamics calculations (using the empirical $ReaxFF_{SiO}^{GSI}$ potential, where the vibrational energy of recombined molecules is analyzed. As seen in Fig. 9, a vibrational energy corresponding to quantum level v=8 is the most probable state. All current macroscopic flow models assume that molecules leave in the ground vibrational level (v=0). Clearly, the results in Fig. 8 contradict this assumption and there is also supporting evidence of recombination into vibrationally excited states in the computational chemistry literature. If molecules do in-fact leave the surface with significant vibrational energy, this may lower the heat flux to the surface compared to the equilibrium assumption where all vibrational energy is deposited to the surface (i.e. when molecules leave in state v=0).

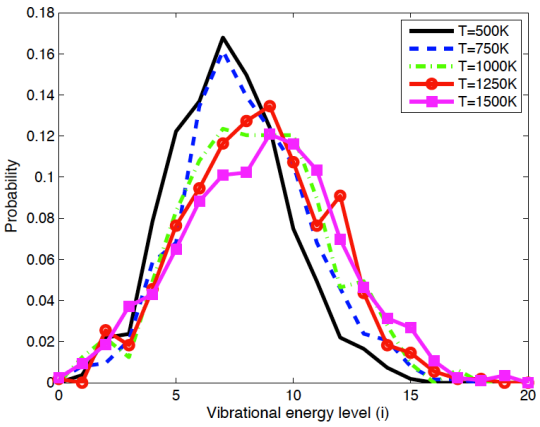

Figure 9: Vibrational energy states of recombined molecules predicted by Molecular Dynamics.

We therefore performed direct simulation Monte Carlo (DSMC) calculations to see how important this effect might be. As detailed below, we found that the vibrational state of recombined molecules has a very small effect on the boundary layer and the overall heat flux to the surface. This is also consistent with the experimental results described in upcoming sections.

Specifically, we chose hypersonic flow conditions with near-complete dissociation and also used a recombination probability at the upper-limit reported in the literature. This ensures that if vibrational accommodation effects are important, they will be clearly evident in such a flow. Five-species air flow over a circular cylinder was simulated, with conditions of 11km/s velocity at an altitude of approximately 75km. The flowfield is shown in Fig. 10a and the species concentrations along the stagnation line are shown in Fig. 10b. As seen in Fig. 10b, both nitrogen and oxygen fully dissociate in the shock layer, and due to the high recombination probability (0.01), significant recombination into molecular oxygen and nitrogen is evident near the stagnation point (inset of Fig. 10b).

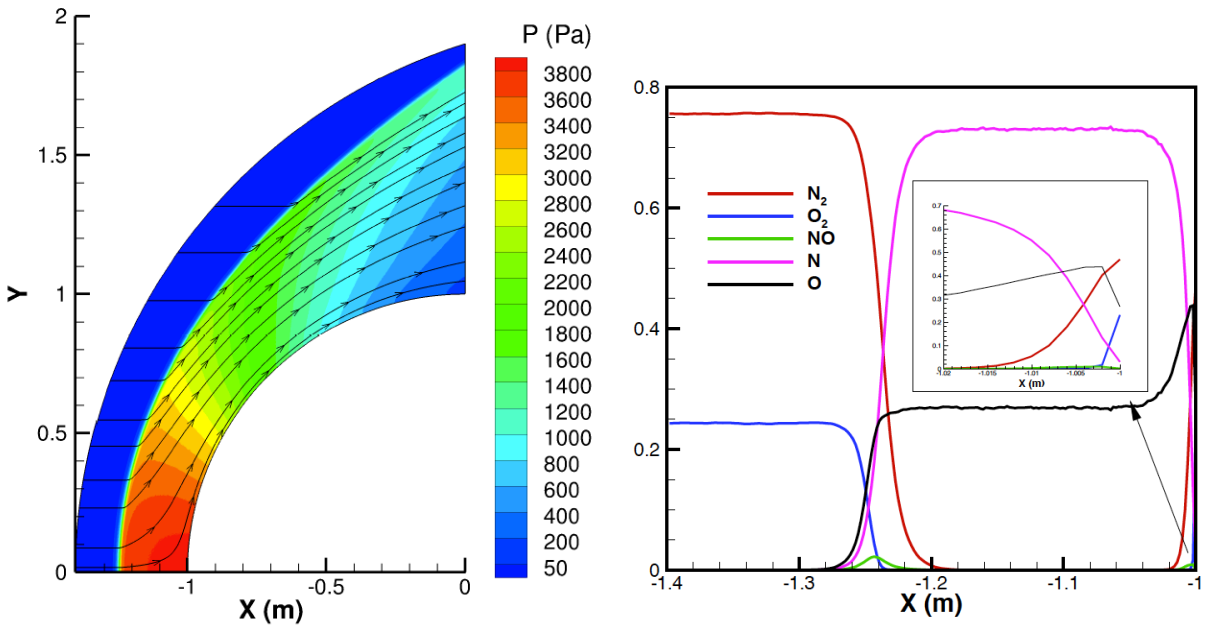

Figure 10: (a) Pressure contours and streamlines for hypersonic flow over a cylinder, (b) species concentrations along the stagnation streamline.

The heat flux to the cylinder surface (vs. angle around the cylinder, θ) is shown in Fig. 11 for cases with/without surface recombination. Clearly, the heat flux due to both oxygen and nitrogen increases significantly when surface recombination is enabled (as expected). However, the purpose of this study is to determine what effect (if any) the *vibrational state* of recombined molecules has on the overall solution and heat flux.

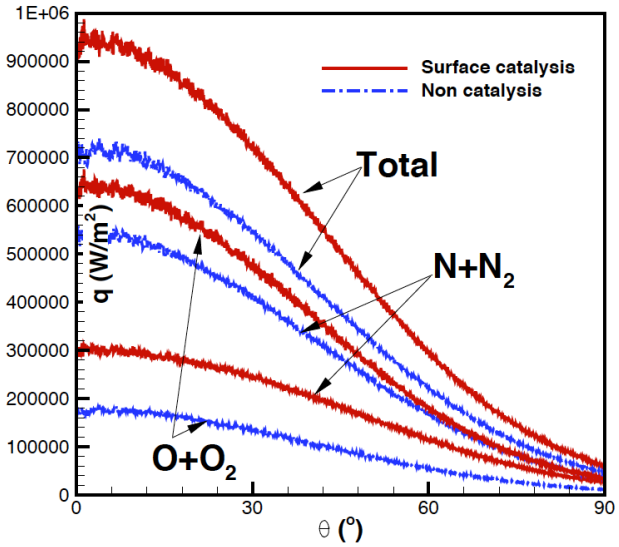

Figure 11: Heat flux contributions with and without surface recombination reactions.

To study this, we ran matching simulations where in one case all molecules deposit all vibrational energy to the surface and leave in state v=0, and the second case where all molecules leave the surface in state v=8 (approximately corresponding to the MD results from Fig. 9 above). As seen in Fig. 12a, as expected, the heat-flux contribution from recombination collisions (producing O_2) decreases when molecules leave the surface in state v=8. However, what we find is that this excess vibrational energy enters the boundary layer flow and is quickly spread throughout the gas through gas-phase collisions. For example, this vibrational energy is transferred to translational energy and, in particular, to the translational energy of O atoms. This leads to an increase in heat-flux due to the O atom collisions with the surface. As seen in Fig. 12b, the total heat flux remains essentially unchanged. We conclude that even if significant vibrational energy is carried into the boundary layer by recombined molecules, this

energy is quickly transferred to other energy modes in the gas, and deposited back to the surface. Since this was a conservative estimate of the effects of vibrational energy accommodation, we expect most flow conditions of interest (as well as the flow tube experiments performed for this project) to involve very little effect due to vibrational energy accommodation.

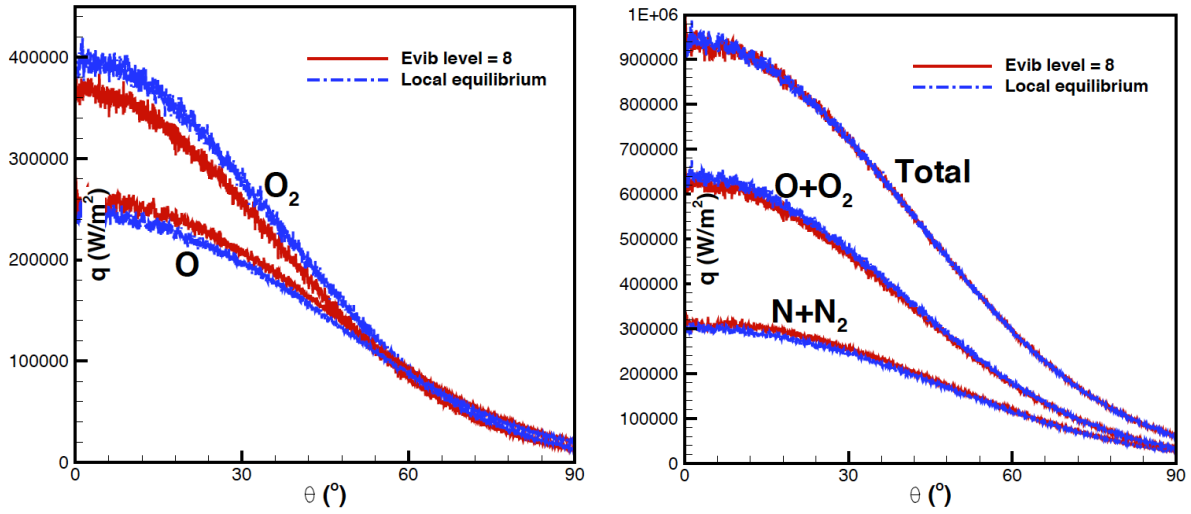

Figure 12: (a) Effect of vibrational energy accommodation to the heat flux contributions from molecular and atomic species, (b) Effect of vibrational energy accommodation to the overall surface heat flux.

Finally, it is important to note that the new computational chemistry methods and results developed in this project (the potential energy surface discussed above) should be capable of precisely characterizing vibrational energy accommodation. Therefore, a much more accurate version of Fig. 9 could be produced. Even if vibrational energy accommodation may not be important for high-density boundary layer flows typical of hypersonic conditions, these results could be important for lower density flows (high-altitude and free-molecular flows) and surface experiments performed in vacuum conditions (i.e. molecular beam experiments).

6. Experimental Verification of Recombination into Electronically Excited O_2

The most important experimental result of this project is the measurement of $O_2(a^1\Delta g)$ ($v = 0$) formation by catalytic O-atom surface recombination on the walls of a fused quartz flow tube reactor at room temperature. Resonance-enhanced multi-photon ionization (REMPI) was used to detect $O_2(a^1\Delta g)$ ($v = 0$) downstream of a nitrogen discharge flow titrated with nitric oxide to introduce oxygen atoms. A calibration procedure based on ozone photodissociation was developed to quantify $O_2(a^1\Delta g)$ ($v = 0$) REMPI signals. Partial pressures of $O_2(a^1\Delta g)$ ($v = 0$) in the range of 4.6 to 10 mTorr were measured in the REMPI cell for O atom partial pressures of 1.3 to 2.9 mTorr atomic oxygen introduced at the titration port. A simple chemical model demonstrates that measured $O_2(a^1\Delta g)$ pressures cannot be explained by gas-phase chemistry alone and must involve O-atoms participating in surface reactions. The complete findings from this study, including the results for $O_2(a^1\Delta g)$ ($v = 1$), can be found in our journal paper [3].

We also performed experiments to look for vibrationally excited singlet O_2 in our flow system, by using (2 + 1) REMPI in the $d^1\Pi g–a^1\Delta g(3,1)$ band to try to detect $O_2(a^1\Delta g)$ ($v = 1$). By comparing REMPI signals from O_3 photodissociation (where vibrationally excited $O_2(a^1\Delta g)$ is

known to form) with signals in our flow system, we conclude that an upper limit for $O_2(a^1\Delta g)$ (v = 1) partial pressure is 1/5 of the $O_2(a^1\Delta g)$ (v = 0) partial pressure. This result indicates that either little $O_2(a^1\Delta g)$ (v = 1) is produced by surface recombination, or that collisional deactivation of $O_2(a^1\Delta g)$ (v = 1) by (primarily) O-atoms in our system is sufficiently fast to deplete the gas-phase $O_2(a^1\Delta g)$ (v = 1) population to these low levels.

We then began exploring the detection of ground-state O-atoms and O_2 molecules in our flow system using REMPI schemes. We explored correlations between the variation of O-atom, ground-state O_2 and singlet O_2 populations as a function of titration, pressure, and flow conditions. Figure 13 shows results from this experiment, where the REMPI cell pressure and the O-atom partial pressure at the titration port are kept fixed, while the bulk flow speed is varied from about 3.4 to 8.1 m/s. As the flow speed increases, more O atoms make it to the REMPI cell and less ground-state O_2 is formed, consistent with the idea that there is less time for surface chemistry to impact gas composition between the titration port and the REMPI cell at higher flow rates.

However, the singlet O_2 signal *increases* with faster flow speeds. *This result can only be explained if reducing the flow time lowers the $O_2(a^1\Delta g)$ quenching rate more than the $O_2(a^1\Delta g)$ production rate on the surface.* Figure 13 shows the variation of O-atom, ground-state O_2, and singlet O_2 REMPI signals (i.e., surrogates for number density) as a function of gas velocity at a fixed REMPI cell pressure and O-atom partial pressure at the titration port.

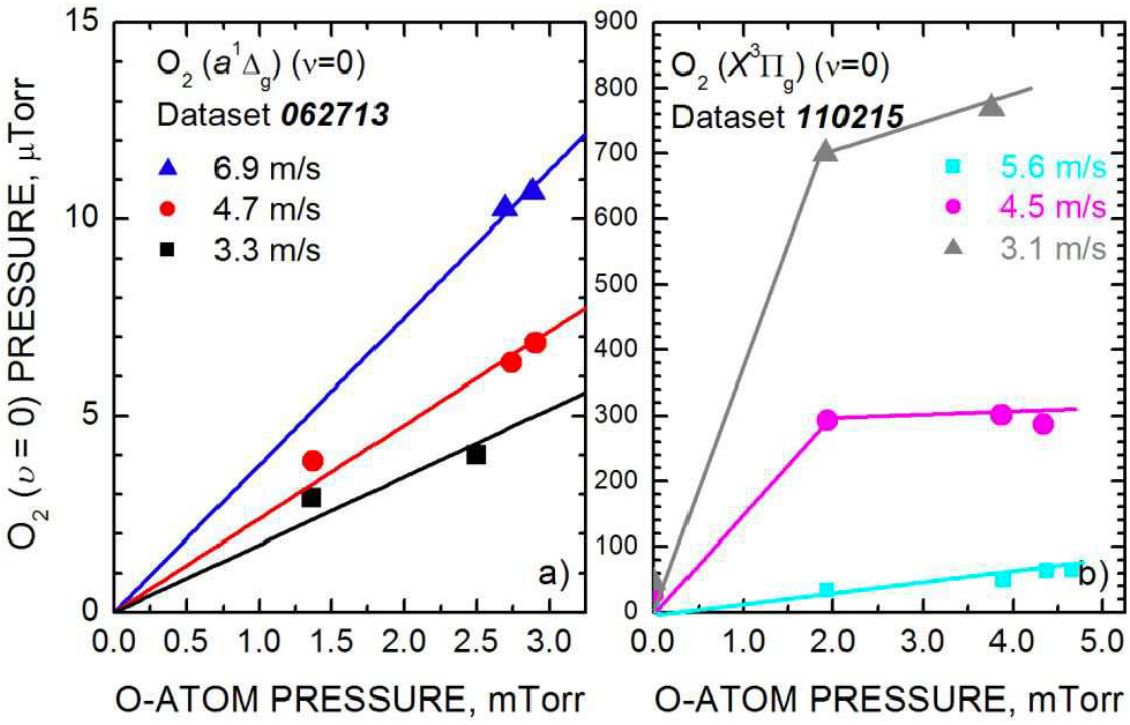

Figure 13: Variation of O_2 (v=0) pressure for the singlet state (Panel A) and the ground state (Panel B).

Here, Panel A is reproduced from our journal publication [3] showing the quantified $O_2(a^1\Delta g)$ (v = 0) velocity response as a function of the O-atom pressure. Panel B shows the quantified ground

state, $O_2(X^3\Sigma_g^-)$ ($\boldsymbol{\nu}$ = 0), from O-atom recombination. Of note, the singlet state increases for higher velocity, while the ground state decreases. Again, this result can only be explained if reducing the flow time lowers the $O_2(a^1\Delta g)$ quenching rate more than the $O_2(a^1\Delta g)$ production rate on the surface. It is also interesting to note that the ground state formation seems to approach a constant conversion percentage above 2.0 mTorr of O-atom pressure. For smaller velocities, we also observe an order of magnitude more ground state than that detected at the higher velocity.

We can use the quantification of $O_2(\boldsymbol{\nu} = 0)$ to estimate the upper limit of the relative population of O2($\boldsymbol{\nu}$ = 1). The Maxwell-Boltzmann population for ($\boldsymbol{\nu}$ = 1) is 0.056% of the (ν = 0) population, leading to an estimate of less than 450 nTorr of ($\boldsymbol{\nu}$ = 1) formation. This, of course, assumes a thermal distribution of oxygen molecules in the gas flow. This result is consistent with the findings from the DSMC simulations presented in Section 5 above. Any $O_2(\boldsymbol{\nu} = 1)$ rapidly drops to $O_2(\boldsymbol{\nu} = 0)$ through non-reactive collisional energy transfer in the gas-phase, rapidly reaching Boltzmann populations under the conditions considered.

7. Flow Modeling and Quantification of the $O_2(a^1\Delta g)$ Production Rate

To interpret the optical diagnostic measurements taken in the flow tube experiments discussed above, and quantify the production of electronically excited O_2, a model for the experimental flow conditions including finite rate gas-phase and gas-surface reactions was required.

To evaluate the potential contributions of gas-phase and surface reactions on the $O_2(a^1\Delta g)$ partial pressure downstream of the titration port, a simple isothermal, constant pressure, plug flow chemistry model was assembled. This model is used to compute species concentrations in our gas mixtures at a reaction time corresponding to the flow time between the titration port and the REMPI cell. The flow times for the high flow and low flow conditions are approximately 230 and 500 ms , respectively. Table I lists the gas phase reactions considered and their room temperature rate coefficients. The references and further details are contained in our journal paper [3] from the referenced sources. Reactions R1 and R3 are sufficiently exothermic that they can produce $O_2(a^1\Delta g)$ as a product. Reactions R7-R11 remove the $O_2(a^1\Delta g)$ from the gas phase by chemical conversion or collisional deactivation.

Heterogeneous O-atom recombination to O_2 and N-atom recombination to N_2 are modeled as two independent surface reactions that proceed with specified efficiencies γ_O and γ_N, where the efficiencies are defined as the fraction of atom collisions with the surface that result in removal of the atom from the gas-phase. The effective heterogeneous reaction rates are then given (in s^{-1}) by $k_{wO} = \gamma_O \langle V \rangle_O / d$ and $k_{wN} = \gamma_N \langle V \rangle_N / d$, where $\langle V \rangle$ is the average thermal speed and d is the inner diameter of the flow tube. Typically reported surface recombination efficiencies (γ) for room temperature O-atom and N-atom recombination on quartz and silica are on the order of 10^{-4} to 10^{-5}. Surface recombination of atomic oxygen is also sufficiently exothermic to produce $O_2(a^1\Delta g)$, however, the formation rate is unknown. Combining the flow model with the experimental data is what enables us to infer the formation rate of $O_2(a^1\Delta g)$ due to surface recombination reactions.

Table I: Gas-phase reactions, surface reactions, and room temperature rate coefficients. Bimolecular and termolecular rate coefficients are in units of cm^3 $molecule^{-1}$ s^{-1} and cm^6 $molecule^{-2}$ s^{-1}, respectively.

	Reaction	Rate Coefficient	Reference
R1	$O + O + N_2 \rightarrow (O_2, O_2(^1\Delta_g)) + N_2$	$k_1 = 2.7\times10^{-33}$	6
R2	$O + O_2 + N_2 \rightarrow O_3 + N_2$	$k_2 = 6.0\times10^{-34}$	9
R3	$O + O_3 \rightarrow (O_2, O_2(^1\Delta_g)) + (O_2, O_2(^1\Delta_g))$	$k_3 = 8.0\times10^{-15}$	9
R4	$O + N + N_2 \rightarrow NO + N_2$	$k_4 = 1.0\times10^{-32}$	23
R5	$N + N + N_2 \rightarrow N_2 + N_2$	$k_5 = 4.4\times10^{-33}$	23
R6	$N + NO \rightarrow N_2 + O$	$k_6 = 3.0\times10^{-11}$	9
R7	$O_2(^1\Delta_g) + O \rightarrow O_2 + O$	$k_7 < 2.0\times10^{-16}$	9
R8	$O_2(^1\Delta_g) + O_3 \rightarrow O_2 + O_2 + O$	$k_8 = 3.8\times10^{-15}$	9
R9	$O_2(^1\Delta_g) + N \rightarrow NO + O$	$k_9 < 9.0\times10^{-17}$	9
R10	$O_2(^1\Delta_g) + O_2 \rightarrow O_2 + O_2$	$k_{10} = 1.7\times10^{-18}$	9
R11	$O_2(^1\Delta_g) + N_2 \rightarrow O_2 + N_2$	$k_{11} < 1.0\times10^{-20}$	9
W1	$O + O + wall \rightarrow (O_2, O_2(^1\Delta_g)) + wall$	k_{wO}	See text
W2	$N + N + wall \rightarrow N_2 + wall$	k_{wN}	See text
W3	$O_2(^1\Delta_g) + wall \rightarrow O_2 + wall$	$k_{wO2\Delta}$	See text

Importantly, we have also included a similar heterogeneous reaction rate expression, $k_{w\text{-}O2\Delta} = \gamma_{O2\Delta} \langle V \rangle_{O2\Delta}/d$, for the collisional deactivation of $O_2(a^1\Delta g)$ (i.e. quenching) to the ground state by the tube surface. The surface deactivation efficiency of $O_2(a^1\Delta g)$, ($\gamma_{O2\Delta}$), on quartz and silica is reported to be on the order of 10^{-4} to 10^{-5} at room temperature.

Simulations with this simple chemistry model produce the following conclusions. First, surface recombination reactions must be involved in the production of $O_2(a^1\Delta g)$ because gas-phase reactions alone cannot produce the experimentally measured $O_2(a^1\Delta g)$ pressures. Even with unrealistic limits that maximize gas-phase $O_2(a^1\Delta g)$ production, specifically $\gamma_O=0$, $\gamma_{O2\Delta}=0$ and 100% production yield for reactions R1 and R3, the computed partial pressures in the REMPI cell are smaller than the measured values for every condition tested. We therefore confirm that surface recombination reactions, between atomic oxygen and a quartz surface, produce significant molecular oxygen in the first electronically excited state.

Second, the rate coefficients for the gas-phase quenching reactions R7-R11 are very small and they have essentially no effect on $O_2(a^1\Delta g)$ pressures under our experimental conditions; however; surface quenching of $O_2(a^1\Delta g)$by reaction W3 can impact $O_2(a^1\Delta g)$ pressures for deactivation efficiencies of ~10^{-5} and higher.

Third, the scaling behavior between O-atom pressure at the titration port and $O_2(a^1\Delta g)$ pressure in the REMPI cell is well reproduced by the model. For a given flow condition, any set of model inputs (surface recombination and deactivation coefficients and $O_2(a^1\Delta g)$ production yields for reactions R1, R3, and W1) that reproduces the measured $O_2(a^1\Delta g)$ pressure at one titration level, also does so at other titration levels.

Fourth, and importantly, significant collisional deactivation of $O_2(a^1\Delta g)$ by the tube surface is required to reproduce the experimental result that $O_2(a^1\Delta g)$ pressures decrease rather than increase with longer flow times at a fixed titration port O-atom pressure.

Finally, it is only when $O_2(a^1\Delta g)$ surface production yields reach 10% *and* collisional deactivation (quenching) efficiency reaches values greater than $6x10^{-4}$ that the model reproduces the experimental trends at all flow conditions.

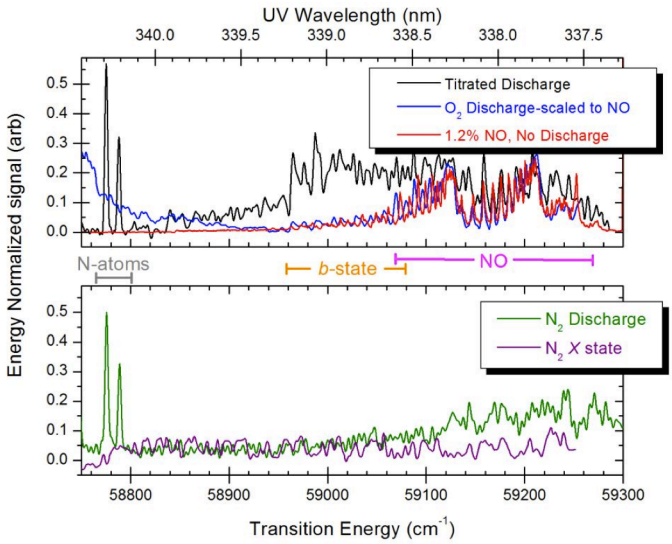

Figure 14: Spectroscopic scans in the region of the transitions for $d\ ^1\Pi_g - b\ ^1\Sigma^+_g$ (2,0). Top Panel: the titrated N_2 discharge(~50% end-point)[black], the O_2 discharge [blue] scaled to NO ground state [red]. Bottom Panel: The N_2 discharge (green) compared to the N_2 ground state [purple]. Molecular transitions identified in labels and ranges shown between the plots.

8. Experimental Detection of Recombination into the 2nd Electronically Excited State of O_2

Focus then shifted to the production of $O_2(b^1\Sigma g^+)$ by catalytic O-atom surface recombination on the walls of a fused quartz flow tube reactor at room temperature. We used resonance enhanced multi-photon ionization (REMPI) to detect $O_2(b^1\Sigma g^+)(\boldsymbol{v} = 0)$ downstream of a nitrogen discharge flow titrated with nitric oxide to introduce oxygen atoms. A submission to the *AIAA Journal of Thermophysics and Heat Transfer* is in preparation. Experiments to detect $O_2(b^1\Sigma g^+)(\boldsymbol{v} = 0)$ in our flow system due to recombination were performed by using a (2 + 1) REMPI transition in the $d\ ^1\Pi_g$-$b^1\Sigma g^+$(2,0) and (3,0) bands. The (2-0) transition overlaps with previously detected NO peaks that show strong signals. Although we operate under the titration endpoint, there exists the possibility that unreacted N-atoms can recombine in the gas phase with gas-phase O-atoms or via extraction from adsorbed O-atoms. We therefore studied the (3-0) transition in the region depicted in Fig. 14 that is identified with the orange text (see Fig. 15 for line assignments). Here, the N_2 titrated discharge (black line) is compared to the scaled NO ground state scan (red). The titrated discharge shows very strong REMPI signals between 58975 cm^{-1} and 59050 cm^{-1} that are not associated with NO. Further comparisons to the un-titrated N_2 discharge (green line) and N_2 ground state (purple line), show no contributions to the peaks identified as belonging to the *b*-state.

Turning to Fig. 15, which directly compares the titrated discharge with the O_2 discharge, provides identification of the transitions for the *b*-state, indicated by the colored tics with

associated Segment branch assignments. The three peaks labeled with asterisks are observed most strongly in the titrated discharge, and match to within 0.01 cm^{-1} to the shifts reported for the J=14, 16, and 18 Segment b branches. At this time, it is unclear why the Segment b S-branch appears to be the strongest detectible transition.

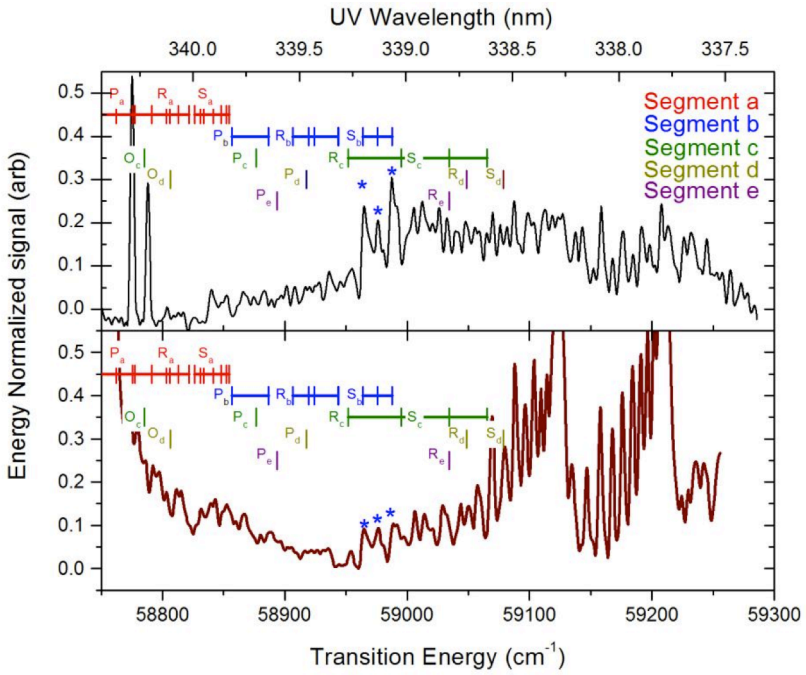

Figure 15: A comparison of the titrated nitrogen discharge and an O_2 discharge. The top panel shows the titrated discharge and is overlaid with the $d\,^1\Pi_g - b\,^1\Sigma_g^+$ (3,0). The peaks identified with an asterisk are consistent with the Segment b branch for J=14,16,17. The bottom panel compares the O_2 discharge, and these Segment b-branches are apparent here, as well. With the O_2 discharge, the Segment a-branch becomes more apparent.

The two peaks at lower energy are identified as N-atom transitions as they are seen only when operating the N_2 discharge. It is thought that they are from residual N-atoms that are not consumed by the titration.

HIGH LEVEL SUMMARY

The technical accomplishments of the project are best summarized by the **point-to-point summary** listed at the beginning of this report. Here, the primary PI (Schwartzentruber), provides a high-level summary of the important project results with an emphasis on how the results impact the field of aerothermodynamics and hypersonic vehicle design.

Upon completion of this project, we now have a fundamental understanding of oxygen recombination reactions on SiO_2 surfaces (amorphous and crystalline surfaces) at high temperature. These recombination reactions occur only on surface defects where dangling bonds provide energetically favorable pathways for atomic oxygen to recombine into molecular oxygen. These reactions are highly exothermic and therefore transfer energy to the surface ("chemical" heat flux). In fact, there is sufficient energy released in these reactions that product molecules leave the surface in vibrationally and even electronically excited states.

We now understand that these reactions have no energy barrier. In other words, these are non-activated processes that occur independent of the gas-surface temperature. Rather, these reactions simply occur (a downhill reaction process) in the presence of both atomic oxygen and these surface defects. The higher the density of surface defects, the higher the reactivity of the surface, and the lower the density of surface defects, the lower the reactivity of the surface. This was a somewhat unexpected result of the project, however in hindsight, is perfectly consistent with existing experimental data in the literature for surface temperatures below 1000K. In contrast, all current finite-rate oxygen-silica models used in the aerothermodynamic community assume an activated process. We conclude that this assumption is incorrect and that these reactions should be modeled with no activation energy. The reactivity of a silica surface may still depend on surface temperature above 1000K (as limited experimental data seems to suggest). If so, this increased reactivity is more likely a result of an increase surface defect density as the SiO_2 surface approaches its phase-change (temperature/pressure) threshold, rather than a result of an activated reaction mechanism.

We note that the empirical interatomic potential, $ReaxFF_{SiO}^{GSI}$, although qualitatively accurate, was not able to accurately determine the energy barriers of interest (or lack thereof). This is despite the fact that $ReaxFF_{SiO}^{GSI}$ was trained specifically to subsets of the electronic structure data. The $ReaxFF_{SiO}^{GSI}$ predicted spurious energy barriers (likely due to the empirical fitting strategies employed) and was not yet capable of investigating excited electronic energy levels (non-adiabatic processes). Although empirical potentials may not be sufficiently precise for determining activation energies for gas-surface interactions, we found that the surface defects are "chemically isolated". Fortunately, this means that small cluster models of the defects are physically representative and can be accurately modeled with electronic structure calculations.

Using accurate electronic structure calculations, we were able to determine the precise atomic configurations of the surface defects, and study the energy pathways (reaction profiles) for atomic oxygen recombining into molecular oxygen on these defects. The exhaustive set of electronic structure calculations even included low-lying electronic energy levels. The calculations predicted that the recombination reaction has no energy barrier, and furthermore that vibrationally excited and electronically excited molecular oxygen should be produced.

Through direct simulation Monte Carlo (DSMC) studies, we determined that the vibrational energy level of recombined molecules has a negligible impact on the overall heat flux delivered to a hypersonic vehicle surface. Even though significant vibrational energy is carried away form the surface by recombined molecules, this energy is quickly transferred (through collisional processes) to other energy modes (mainly translational energy) within the boundary layer gas. This energy is then transferred back to the surface through convective heating from the boundary layer.

In contrast, if electronic energy is carried away from the surface by recombined molecules, this energy is not expected to be transferred within the boundary layer due to the very long timescales of gas-phase electronic energy quenching reactions. In principle, this energy could be carried away from the surface, thereby reducing the heat flux to the surface. The experimental measurements performed for this project confirmed recombination into the first and second electronically excited states of molecular oxygen. Specifically, the experimental measurements combined with flow modeling determined that $1/10^{th}$ of surface recombination reactions produce oxygen in the first electronically excited state. However, a crucial finding of the experiments (and associated flow modeling) was that quenching of electronic energy due to collisions between excited oxygen and the silica surface, is more probable than the production of electronic energy. Production only occurs at surface defects through the recombination reactions, whereas quenching can occur on non-defective portions (i.e the majority) of the surface. This result could be very important for computational modeling of ground-based high-enthalpy facilities. In expanding a high temperature gas to produce the high-enthalpy, high-speed flow conditions, the flow within the test-sections of many facilities may contain electronically excited oxygen. If this energy is efficiently quenched on the surface, then this should be included in computational simulations of the facility. If not, a non-negligible contribution to the heat flux may be missing from the computations. This could then affect the interpretation of other phenomena of interest.

In summary, we now have a fundamental understanding of oxygen recombination reactions on silica surfaces. In principle, the detailed data produced by this project could be used in the future to tailor surfaces or surface coatings. However, the fact that such SiO_2 surfaces often form during flight due to oxidation of underlying silica-forming TPS, makes such tailoring difficult to realize. Also, even though electronic energy is carried away from the surface with non-negligible efficiency, it is quenched on the surface at higher efficiency. Therefore, at this point, it is also difficult to realize a surface design that can exploit recombination into electronically excited states. Furthermore, the project's conclusions regarding the lack of an energy barrier for oxygen-silica recombination reactions and the efficiency of electronic energy quenching on silica surfaces should immediately be used in aerothermodynamic modeling.

Future work should focus on understanding what happens above 1000K. This is much more difficult from a computational chemistry standpoint, as the structure of the surface itself (at the atomic level) during phase change is complex and currently unknown. One promising path forward is molecular beam experiments, where a well characterized O atom source can be directed at a material sample heated to high temperature and all scattered products quantified in detail. Such experiments could explore surface temperatures well above 1000K and could be performed on more chemically complex surface coatings compared to pure SiO_2.

REFERENCES:

There are many references associated with the computational and experimental techniques. These are listed in detail in our journal papers, particularly [1, 2, and 3]. All results in this report have been published.

1.

1. Report Type

Final Report

Primary Contact E-mail

Contact email if there is a problem with the report.

schwart@umn.edu

Primary Contact Phone Number

Contact phone number if there is a problem with the report

612-625-6027

Organization / Institution name

University of Minnesota

Grant/Contract Title

The full title of the funded effort.

Reduced Heat Flux Through Preferential Surface Reactions Leading to Vibrationally and Electronically Excited Product States

Grant/Contract Number

AFOSR assigned control number. It must begin with "FA9550" or "F49620" or "FA2386".

FA9550-12-1-0486

Principal Investigator Name

The full name of the principal investigator on the grant or contract.

Thomas E. Schwartzentruber

Program Manager

The AFOSR Program Manager currently assigned to the award

Dr. Michael Berman

Reporting Period Start Date

09/30/2012

Reporting Period End Date

11/30/2015

Abstract

Instead of characterizing a hypersonic flight environment and then selecting an appropriate thermal protection system (TPS) that can survive the environment, it would be a significant technological step forward if the TPS could be engineered to alter the hypersonic flight environment itself (i.e. the boundary layer). A critical aspect of such a strategy is control over energy deposition pathways during catalytic recombination of dissociated air species on TPS surfaces. Experiments with laser-based diagnostics were used to simultaneously measure the loss of oxygen atoms and the production of oxygen molecules in the ground and electronically excited states as a partially dissociated oxygen flow interacts with a silica surface. Flow models were constructed and numerical calculations were performed to interpret the experimental data. New computational chemistry approaches, capable of modeling nonadiabatic oxygen interactions (electronically excited interactions) with surface defects, were developed. Through such computational chemistry modeling we determined precisely how and why such excited-state molecules are produced, by determining the specific silica defects and reaction pathways that are responsible.

Distribution Statement

This is block 12 on the SF298 form.

Distribution A - Approved for Public Release

Explanation for Distribution Statement

If this is not approved for public release, please provide a short explanation. E.g., contains proprietary information.

SF298 Form

Please attach your SF298 form. A blank SF298 can be found here. Please do not password protect or secure the PDF The maximum file size for an SF298 is 50MB.

Cover_Page.pdf

Upload the Report Document. File must be a PDF. Please do not password protect or secure the PDF . The maximum file size for the Report Document is 50MB.

Final_Report_FA9550-12-1-0486_Schwartzentruber.pdf

Upload a Report Document, if any. The maximum file size for the Report Document is 50MB.

Archival Publications (published) during reporting period:

BOOK CHAPTER:
Jochen Marschall, Matthew MacLean, Paul E. Norman, and Thomas E. Schwartzentruber, Hypersonic Nonequilibrium Flows: Fundamentals and Recent Advances Chapter 6: Surface Chemistry in Nonequilibrium Flows, Progress in Astronautics and Aeronautics, Volume 247, AIAA 2015. http://dx.doi.org/10.2514/5.9781624103292.0239.0328

ARTICLES:
[1] Paneda, R.M., Paukku, Y., Duanmu, K., Norman, P., Schwartzentruber, T.E., and Truhlar, D.G., "Atomic Oxygen Recombination at Surface Defects on Reconstructed (0001) α-Quartz Exposed to Atomic and Molecular Oxygen", J. Phys. Chem. C (2015), 119, pp. 9287-9301.

[2] Norman, P., Schwartzentruber, T.E., Leverentz, H., Luo, A., Paneda, R.M., Paukku, Y., and Truhlar, D.G., "The Structure of Silica Surfaces Exposed to Atomic Oxygen", J. Phys. Chem. C (2013), 117, pp. 9311-9321.

[3] "Singlet Molecular Oxygen Formation by O-atom Recombination on Fused Quartz Surfaces", by J. D. White, R. A. Copeland, and J. Marschall, Journal of Thermophysics and Heat Transfer, 29, No.1, pp. 24-36. January-March 2015.

[4] Schwartzentruber, T.E., Poovathingal, S., and Stern, E.C., "Molecular Simulation of Oxygen Reactions with Realistic Carbon and Silica Surfaces at High Temperature", AIAA Paper 2015-3567, July 2015, presented at the 20th AIAA International Space Planes and Hypersonic Systems and Technologies Conference, Glasgow, Scotland.

[5] Schwartzentruber, T.E., Poovathingal, S., and Stern, E.C., "Molecular Simulation of Oxygen Reactions with Realistic Silica and Carbon Surfaces at High Temperature", Proceedings of the 8th European Symposium on Aerothermodynamics, European Space Agency, 2015, id.84668, Lisbon, Portugal.

[6] White, Jason D., Richard A. Copeland, and Jochen Marschall. "Singlet O2 Formation by O-atom Recombination on Fused Quartz Surfaces." AIAA Paper 2014-0515, 52nd Aerospace Sciences Meeting. National Harbor, Maryland, 2014.

Changes in research objectives (if any):

Change in AFOSR Program Manager, if any:

Extensions granted or milestones slipped, if any:

AFOSR LRIR Number

LRIR Title

Reporting Period

Laboratory Task Manager

Program Officer

Research Objectives

Technical Summary

Funding Summary by Cost Category (by FY, $K)

	Starting FY	FY+1	FY+2
Salary			
Equipment/Facilities			
Supplies			
Total			

Report Document

Report Document - Text Analysis

Report Document - Text Analysis

Appendix Documents

2. Thank You

E-mail user

Feb 27, 2016 20:59:06 Success: Email Sent to: schwart@umn.edu